HHS Public Access

Author manuscript

Biol Psychiatry Cogn Neurosci Neuroimaging. Author manuscript; available in PMC 2023 September 01.

Effects of smoking status and state on intrinsic connectivity

Sarah W. Yip, PhD[1,*], **Sarah D. Lichenstein, PhD**[2], **Kathleen Garrison, PhD**[1], **Christopher L. Averill, BS**[1,3,5,6], **Humsini Viswanath, MS, MPH**[4], **Ramiro Salas, PhD**[3,6], **Chadi G. Abdallah, MD**[1,3,5,6]

[1]Department of Psychiatry, Yale University School of Medicine, New Haven, CT, USA

[2]Radiology and Biomedical Imaging, Yale University School of Medicine, New Haven, CT, USA

[3]Menninger Department of Psychiatry and Behavioral Sciences, Baylor College of Medicine, Houston, TX, USA

[4]Department of Neuroscience, Baylor College of Medicine, Houston, TX, USA

[5]VA National Center for PTSD—Clinical Neurosciences Division, West Haven, CT, USA

[6]Michael E DeBakey VA Medical Center, Houston, TX, USA

Abstract

Background: Smoking behavior during the first 24 hours of a quit attempt is a significant predictor of longer term abstinence, yet little is known about the neurobiology of early tobacco abstinence. Specifically, the effects of acute tobacco deprivation and reinstatement on brain function—particularly at the level of large-scale network dynamics and assessed across the entire brain—remain incompletely understood. To address this gap, this study uses a mixed within- and between-subjects design to assess the effects of smoking status (yes/no smoker) and state (deprived versus satiated) on whole-brain patterns of intrinsic connectivity.

Methods: Forty-two tobacco smokers participated in resting state fMRI following overnight abstinence (deprived state) and following smoking reinstatement (satiated state, randomized order across participants). Sixty healthy control non-smokers participated in a single resting state scan using the same acquisition parameters. Functional connectivity data were analyzed using both a canonical network-of-interest (NOI) approach and a whole-brain, data driven approach, intrinsic connectivity distribution (ICD).

Results: NOI-based analyses indicated decreased functional connectivity within frontoparietal and salience networks among smokers relative to nonsmokers, as well as effects of smoking state on default mode connectivity. In addition, ICD analyses identified novel between-group differences in subcortical-cerebellar and cortico-cerebellar networks that were largely smoking state dependent.

[*]Address for correspondence: Sarah W. Yip, PhD, 1 Church Street, Suite 731, New Haven, CT, 06510, USA; sarah.yip@yale.edu; Tel: (203) 737 4358.

Author contributions: Dr. Salas designed the study and was responsible for data collection, in collaboration with Dr. Viswanath and Mr. Averill. Drs. Yip, Lichenstein and Abdallah collaborated on the neuroimaging analyses. Dr. Yip wrote the first draft of the manuscript in consultation with Dr. Garrison. All authors assisted in interpretation of data and provided critical feedback on the manuscript.

Conclusions: These data demonstrate the importance of considering smoking state and the utility of using both theory- and data-driven analysis approaches. These data provide much needed insight into the functional neurobiology of early abstinence, which may be used in the development of novel treatments.

Introduction

Tobacco smoking is a primary cause of preventable death and is particularly prevalent among individuals with psychiatric disorders, including other substance use disorders, mood disorders, and schizophrenia(1–3). While evidence-based interventions exist, overall rates of smoking cessation following treatment remain suboptimal(4). Thus, further research to improve existing treatments is needed. Within this context, elucidation of the functional effects of different tobacco use behaviors (e.g., abstinence, reinstatement) and corresponding brain states (e.g., deprivation, satiation) may inform development of novel intervention strategies(5, 6). However, effects of tobacco smoking on brain function—particularly at the level of large-scale network dynamics—remain incompletely understood.

Nicotine acts primarily on nicotinic acetylcholine receptors (nAchRs), which are distributed widely throughout the cortex, subcortex, and cerebellum(7). Consistent with this, prior studies indicate connectivity differences between smokers and nonsmokers within distributed neural networks, typically involving decreased connectivity within 'canonical' networks (e.g., default mode, frontoparietal, salience) among smokers(8). In addition, studies using within-subjects designs to compare networks during nicotine deprivation (e.g., overnight abstinence) versus satiation (i.e., following smoking reinstatement) indicate that patterns of functional connectivity within and between canonical networks differ across smoking states(6, 8). In particular, decreased connectivity between salience and frontoparietal networks, coupled with increased connectivity between the salience and default mode network has been proposed to promote individuals' focus on the internal craving state during acute abstinence(8). Although a number of studies provide partial support for this hypothesis(6, 9, 10), very few studies have concurrently examined connectivity of these key canonical networks during deprived versus satiated states(11, 12). In addition, it is not clear whether connectivity changes represent a restoration to (i.e., return to premorbid levels)—or deviation from (i.e., alteration from premorbid levels)—typical patterns of intrinsic connectivity(13). Here, we use a mixed within- and between-subjects design to assess the effects of smoking state (deprived versus satiated) on intrinsic connectivity comparisons of smokers versus nonsmokers in a data driven manner.

Traditional functional connectivity approaches—including those previously used to study smoking effects(6, 9, 11, 14–16)—require *a priori* selection of seed regions or networks. Although these approaches can provide insights into regional patterns of connectivity, they also have some important limitations. In particular, regions-of-interest defined on the basis of brain atlases or cortical parcellations may actually contain multiple distinct time-courses that are averaged together in traditional seed-based connectivity analyses, yielding potentially inaccurate connectivity estimates(17). Furthermore, limiting analyses to specific regions or networks also precludes the identification of effects in a data-driven, whole-brain manner. To overcome these limitations, we here apply a recently developed approach,

intrinsic connectivity distribution (ICD)(17), to characterize large-scale network dynamics among smokers across deprived and satiated states, and in comparison to a nonsmoking comparison group. Unlike other functional connectivity approaches, ICD requires no specification of seed regions, networks, or connectivity thresholds(17–19) and is therefore an entirely data-driven, whole-brain analysis approach ideally suited for assessment of systems-level effects. However, as clusters identified in whole-brain ICD analyses may reflect both global (distributed) and focal (localized) alterations in connectivity. However, as ICD and similar voxel-to-voxel connectivity approaches compress all connectivity information about a voxel into a single number (in this case, α) any spatial information about which connections primarily contribute to differences in connectivity for that voxel is lost, necessitating follow-up seed-to-voxel connectivity analyses(17, 20). Thus ICD and seed-based approaches may be considered complementary(17).

Based on prior work(6, 8, 12), we anticipated that ICD comparisons would identify distributed between-group differences in connectivity between canonical neural networks (e.g., default mode, executive control/frontoparietal, and salience networks), involving decreased connectivity in smokers relative to nonsmokers, and that these differences would be heightened during deprived versus satiated states. Given this hypothesis, and to facilitate comparisons with prior work, we also conducted a network-of-interest (i.e., non-whole-brain) analysis localized to connectivity within and between these canonical networks. Between-network connectivity was summarized using the resource allocation index, a composite measure defined as the difference in salience network connectivity to frontoparietal versus default mode networks previously implicated in tobacco smoking(12). Further, given the widespread distribution of nAchRs throughout the brain(7), we also hypothesized that ICD would identify effects of smoking state on connectivity within more distributed neural systems; e.g., corticostriatal and corticocerebellar circuits(21, 22).

Methods

Participants and recruitment

Smokers and non-smokers between the ages of 18 and 65 were recruited from the Houston metropolitan area via fliers, newspaper, and Internet advertisements, as in our prior work(23, 24). Smokers were defined as individuals who reported smoking ≥10 cigarettes a day. All participants were pre-screened to rule out non-tobacco substance dependence or MRI contraindications. This included self-report of being healthy, not having a neurological disorder or non-nicotine substance-use disorder. No structured clinical interview or urine toxicology screening was conducted. Smokers currently seeking cessation treatment were also excluded. A total of 114 individuals (53 smokers, 61 nonsmokers) participated in neuroimaging protocols. Following exclusion for excess motion (>.30 mm mean frame-to-frame displacement(25)), incomplete or missing data (e.g., only one scanning session completed for smokers), the final sample included 102 individuals (42 smokers (10 female), 60 nonsmokers (34 female). Smokers and non-smokers were significantly different in age (smokers: 44.64±11.20, non-smokers: 29.27±10.16, $t_{(df=100)}=7.20$, $p<.001$) and the smoking group had significantly fewer female participants ($x^2=8.97$, $p=.003$). Smoking history and dependence were evaluated using the Fagerström Test for Nicotine Dependence (FTND)

(26). Smokers had significant smoking histories, with a mean (±standard deviation) smoking duration of 27.90(±11.90) years, mean cigarettes/day of 16.93(±7.02) and mean FTND scores measured during deprivation of 5.45(±2.04) and of 5.10(±2.00) during satiation. Studies were conducted at Baylor College of Medicine and were IRB approved.

Study design and neuroimaging acquisition

Deprived and satiated scans occurred on separate days (approximately 7 days apart) and individuals were randomly assigned to either deprived first or satiated first order. Consistent with prior work, for the deprived session, smokers were asked to abstain from tobacco smoking and other nicotine-containing products since midnight the previous day of the scanning sessions, which occurred in the morning (27). For the satiated scan, smokers were allowed to smoke *ad libitum* to achieve satiation. Prior to scanning, participants completed self-report assessments of craving and withdrawal and provided CO measurements to confirm smoking state (deprived versus satiated). Withdrawal, craving and stimulation/sedation symptoms were assessed using the Shiffman-Jarvik Withdrawal Questionnaire (SJWQ)(28), a widely used self-report measure. For the satiated session, smokers were asked to come to the lab smoking as usual, and were given the option to smoke before the scan if they feel like doing so. Non-smoking comparison participants were scanned once. Neuroimaging data was acquired during resting state using a 3T MAGNETOM Trio scanner (Siemens). Each MRI session began with a magnetization-prepared rapid gradient echo (MPRAGE) structural scan (160 axial slices, 1× 1×1mm voxels, TE=2.66 ms, TR=1.2s, flip angle=12°, 256×256 matrix). Subjects were then scanned while resting (eyes open or closed) for 5 min (3.4×3.4×4.0mm voxels, TE=40ms, TR=2.0s, flip angle=90°). An “X” was displayed in the screen, but no specific instruction was given except to “let your mind wander”.

Pre-processing

Whole-brain functional connectivity analyses were conducted using the BioImage suite(29–31). Functional data were motion and slice-time corrected using SPM8 (http://www.fil.ion.ucl.ac.uk/spm/). Additional preprocessing was conducted using the BioImage Suite(32) and included linear and quadratic drift correction, smoothing to 6 mm full width half maximum and regression of a 24-parameter motion model (including six rigid-body motion parameters, six temporal derivatives, and these terms squared)(33) and of other covariates of no interest (linear and quadratic drifts, mean cerebral-spinal-fluid (CSF) signal, mean white-matter signal, and mean gray matter signal). Five smokers and 1 non-smoker were excluded for excess motion (>.30 mm mean frame-to-frame displacement(25)). Functional data were temporally smoothed with a Gaussian filter (approximate cutoff frequency=0.12Hz).

Canonical, network-of-interest analyses

To facilitate comparison between this study and prior work using localized network-of-interest based (i.e., non-whole brain) approaches, connectivity within- and between-canonical neural networks (default mode, frontoparietal, salience) was also assessed in a network-specific matter. For these analyses, the Shen 268-node brain atlas was used to define nodes and mean nodal time courses (i.e., average ‘raw’ time course of voxels

within the node) for computation of node-by-node pairwise Pearson's correlations. Fisher's z-transformation was applied to create symmetric 268×268 connectivity matrices, or 'connectomes', comprised of edges representing the connection strength between each pair of nodes(30, 34), with only positive edges retained following removal of the global mean(17, 35). Canonical networks were defined based on prior work using the Shen 268-atlas(36–38). Consistent with prior work using alternative network definition approaches (e.g., independent component analysis)(6), the salience network included bilateral insulae and dorsal anterior cingulate; the frontoparietal network included bilateral frontal and parietal regions; and the default mode included the posterior cingulate and medial frontal regions (Figure 1). Connectivity values for edges corresponding to canonical between-network connections (e.g., z-transformed correlation coefficients corresponding to connectivity between nodes of the salience network to nodes of the frontoparietal network) were summed for each individual participant and used to compute the resource allocation index (RAI), a composite measure formally defined as:

$$RAI = (mean\ \ nodal\ \ connectivity\ \ between\ \ salience\ \ and\ \ frontoparietal\ \ networks) - (mean\ \ nodal\ \ connectivity\ \ between\ \ salience\ \ and\ \ default\ \ mode\ \ networks)$$

Independent (between-group comparisons) and paired (within-group comparison) t-tests were used to compare default mode, frontoparietal, salience and RAI strengths.

Whole-brain ICD analysis

For a complete description of the development and validation of ICD, see (17). During ICD, voxelwise correlations, in which the correlation between the time course of a given voxel and the time courses of every other voxel in the brain is computed, are conducted across the whole-brain. For each voxel, a histogram of the resultant correlations is then constructed to estimate the distribution of connections to a given voxel and this histogram is converted into a survival function fitted with a stretched exponential with unknown variance, α. By modeling the entire connectivity distribution for each voxel in this manner, ICD eliminates the need to specify an arbitrary connection threshold. As α corresponds to the spread of the distribution of connections, high α values indicate high connectivity(39). This is repeated for each gray matter voxel, resulting in a parametric map of α for each participant, where each voxel in the map represents that voxels' correlation to the rest of the gray matter. To facilitate group comparisons, these maps are scaled across participants using a z-score-like normalization, as in prior work(40, 41), and transformed into MNI space using a single transform calculated as the concatenation of the linear transform of connectivity data to 2D anatomical data, the linear transform of the 2D anatomical data to 3D anatomical data, and the nonlinear transform of the 3D anatomical data to MNI space. Concatenation of the independent linear and nonlinear transforms to create a single transform reduces interpolation error(17, 42). Individual participant aligned images are then concatenated for groupwise, whole-brain analyses.

Whole-brain, between-group comparisons of connectivity maps (deprived smokers vs. controls; satiated smokers vs. controls) were conducted using general-linear models with FSL's randomise with 5,000 permutations. Statistical maps were family-wise-error corrected

for multiple comparisons using FSL's threshold-free-cluster-enhancement (TFCE). As two-tailed group comparisons were conducted twice (once to compare smokers during deprivation relative to nonsmokers, once to compare smokers during satiation relative to nonsmokers), results were considered significant at pTFCE<.01, in order to correct for multiple comparisons.

Seed-to-voxel ICD analysis

Clusters identified in whole-brain analyses as having altered connectivity are used as seeds: Voxelwise correlations of mean timecourses for identified clusters (i.e., 'seeds') are calculated for all other grey matter voxels in the brain to create new connectivity maps and entered into groupwise analyses to identify specific connections contributing to connectivity alterations for each cluster. In the case of global alterations (i.e., when connectivity from a given region is altered to the entire brain), seed-to-voxel analyses may not identify a specific region as a primary contributor. However, in the case of focal alterations, seed-to-voxel analyses may identify specific clusters as primary contributors to connectivity alterations. Seed-to-voxel maps were concatenated and entered into groupwise analyses using randomise with 5000 permutations (pTFCE<.05). As seed-to-voxel these analyses by definition are simply used to determine the primary spatial contributors to clusters already identified as reaching whole-brain significance (pTFCE<.01), no additional statistical correction is needed (17).

ICD comparisons across smoking states

To test for within-subject effects of smoking state, intrinsic connectivity values (α) for regions identified in between-group whole-brain and seed-to-voxel analyses were computed for smokers during deprived and satiated states, respectively, and entered into SPSS for within-subject comparisons (paired t-tests). These values were also used to explore relationships between smoking variables (withdrawal, craving) and connectivity values (Pearson's r) and to test for effects of scan order (derived first vs. satiated first) on connectivity values.

Results

Changes in smoking measures

Consistent with the study design, a significant reduction in measured CO (Micro+ Smokerlyzer Monitor, Bedfont Scientific, Kent, England) was observed for smokers during deprived (9.41±6.31 ppm) versus satiated (25.00±15.29 ppm; $t_{(40)}=-9.01$, $p<0.001$) states. These values are consistent with those previously reported among smokers during deprived and satiated states, respectively(43, 44). Self-reported craving levels and withdrawal scores were significantly elevated during deprived versus satiated states (SJWQ craving: $t_{(df=39)}=3.81$, $p<0.001$, SJWQ withdrawal: $t_{(df=39)}=2.50$, $p=0.017$), but SJWQ stimulation/sedation scores were unchanged across states ($t_{(df=39)}=0.18$, $p=0.858$).

Canonical, network-of-interest analyses

Canonical networks and results of primary analyses for these networks are shown in Figure 1. Independent t-tests indicated significantly lower salience network connectivity among

deprived smokers relative to nonsmokers ($t_{(df=95)}$=2.12, p=0.037), however this effect was not significant when assessed using a general linear model including age (F=2.51, p=0.117) or motion (F=1.85, p=0.178) as a covariate. There were no significant between-group differences in frontoparietal, default mode or resource allocation index strengths between deprived smokers relative to nonsmokers.

Independent t-tests indicated significantly lower salience and frontoparietal network connectivity among satiated smokers relative to nonsmokers (salience: $t_{(df=95)}$=2.52, p=0.013; frontoparietal: $t_{(df=95)}$=1.99, p=0.049) but no significant between-group differences in default mode or resource allocation index strengths. These findings were unchanged in follow-up analyses controlling for age (salience: F=5.05, p=0.027; frontoparietal: F=4.30, p=0.041). However, following inclusion of motion as a covariate, differences in frontoparietal networks were no longer significant (F=2.73, p=0.107).

Paired t-tests within smokers indicated decreased default mode connectivity during deprived versus satiated states ($t_{(df=38)}$=−2.25, p=0.03), but no differences in salience, frontoparietal or resource allocation index strengths. However, this effect was no longer significant when assessed using a general linear model including motion as a covariate (F=2.07, p=0.159). There were no significant associations between canonical network measures and craving or withdrawal indices during deprived or satiated states. There were no main or interaction effects of scan order on canonical network measures. Post-hoc analyses of individual RAI components indicated no significant between-group differences or differences between smoking states in salience-default mode, salience-frontoparietal or default mode-frontoparietal connectivity strengths.

Whole-brain ICD comparisons of smokers versus nonsmokers

ICD comparisons identified four clusters for which whole-brain connectivity was increased (i.e., clusters in which connectivity from each voxel to every other voxel of the brain was increased) in smokers during deprivation, relative to nonsmokers (pTFCE<.01, k>20, Table 1, Figure 2a-b). The first cluster encompassed regions of the left hippocampus, parahippocampal gyrus, amygdala, temporal pole, and bilateral regions of the anterior cerebellum and left posterior cerebellum (details in Table 1). The second and third clusters were located within the right and left cerebellum, respectively. The fourth cluster was located within the left caudate. These findings were unchanged in follow-up analyses controlling for motion and age. Additional follow-up analyses indicated no significant effect of scan order on connectivity within the identified clusters.

Follow-up seed-based analyses from the right cerebellum indicated (a) increased connectivity within a single cluster encompassing distributed areas of the left and right cerebellum extending into the left brainstem and bilateral occipital and temporal regions and (b) decreased connectivity to bilateral anterior cingulate, medial prefrontal cortex and right striatum (caudate, accumbens) medial prefrontal anterior cingulate and striatal regions among deprived smokers relative to controls (Table 1, Figure 3a). Seed-based analyses from the left cerebellar cluster indicated (a) increased connectivity within a single cluster encompassing distributed areas of the left and right cerebellum extending into the left brainstem and occipital and temporal regions and (b) decreased connectivity to bilateral

subgenual cingulate and striatal (caudate) regions (Figure 3c) among deprived smokers relative to controls. These findings were unchanged in follow-up analyses controlling for motion and age. Seed-based connectivity analyses from the left hippocampus or caudate clusters did not identify any specific regions as primary contributors to observed whole-brain alterations in connectivity for these clusters (pTFCE<.05).

ICD comparisons across smoking states

Although we applied ICD to compare patterns of connectivity between nonsmokers and smokers in both deprived and satiated states, there were no significant whole-brain differences in connectivity for smokers in the satiated state relative to nonsmokers (pTFCE<.01). However, paired t-tests within smokers indicated significant effects of smoking state on connectivity within regions identified in the whole-brain comparisons of smokers vs. nonsmokers (reported above; shown in Figure 2c-d) involving increased left hippocampal ($t_{(df=40)}$=3.38, p=0.002) and bilateral cerebellar (left: $t_{(df=40)}$=3.49, p=0.001; right: $t_{(df=40)}$=4.73, p<0.001) connectivity during deprivation versus satiation, but no significant changes in left caudate connectivity ($t_{(df=40)}$=1.84, p=0.074). These findings were unchanged in follow-up analyses controlling for between-scan differences in residual motion.

Paired t-tests within smokers also indicated significant effects of smoking state on connectivity within regions identified in the seed based analyses (reported above; shown in Figure 3b, 3d-g) including stronger within-cerebellar connectivity (right: $t_{(df=41)}$=3.23, p=0.003; left: $t_{(df=41)}$=4.36, p<0.001), weaker right cerebellar-medial PFC connectivity ($t_{(df=41)}$=−2.60, p=0.01) and weaker left cerebellar-corticostriatal connectivity ($t_{(df=41)}$=−3.33, p=0.002) during deprivation versus satiation, but no significant differences in right cerebellar-corticostriatal connectivity ($t_{(df=40)}$=1.81, p=0.077). These findings were unchanged in follow-up analyses controlling for between-scan differences in residual motion.

ICD relationship to smoking measures

Self-reported craving was significantly associated with connectivity in the right hippocampal cluster during satiated ($r_{(df=41)}$=0.31, p=0.049), but not deprived ($r_{(df=41)}$=0.01, p=0.54) states. Withdrawal scores were significantly associated with connectivity within right hippocampal ($r_{(df=41)}$=0.34, p=0.03) and left cerebellar ($r_{(df=41)}$=0.34, p=0.03) clusters during satiated but not deprived ($r_{(df=41)}$=0.13, p=0.43; $r_{(df=41)}$=0.17, p=0.28) states.

Discussion

Neural changes associated with early nicotine abstinence have been associated with symptoms of withdrawal(45, 46) and nicotine craving(12, 15, 16, 47) and may have important implications for predicting longer-term abstinence, yet little is known about the functional neurobiology of early abstinence and reinstatement. This study used a mixed within- and between-subjects design to assess the effects of smoking status (yes/no smoker) and smoking state (deprived versus satiated) on systems-level patterns of connectivity, using both network-of-interest and whole-brain based approaches. Consistent with prior

studies, network-of-interest based analyses indicated decreased functional connectivity within frontoparietal and salience networks among smokers relative to nonsmokers, as well as effects of smoking state on default mode connectivity. In addition, whole-brain analyses identified novel between-group differences in subcortical-cerebellar and cortico-cerebellar networks that were largely smoking state dependent. Together, these data demonstrate the importance of considering smoking state in between-subject comparisons and the utility of using both theory- and data-driven analysis approaches for assessing large-scale network dynamics, and provide much needed insight into the functional neurobiology of early abstinence and return to smoking(6).

Prior functional connectivity studies of tobacco-use have primarily focused on interactions within and between salience, frontoparietal, and default mode networks(6, 8, 9, 11, 14–16), consistent with theoretical models emphasizing these canonical networks as central to addictions and their treatment(25, 48, 49). Within this framework, the salience network is posited to moderate frontoparietal and default mode connectivity, and, during early abstinence, is theorized to enhance attentional resources to interoceptive states via increased connectivity with default mode versus frontoparietal networks(12, 48). However, contrary to this, we found no evidence for smoking state related alterations in this tripartite relationship, as summarized using the resource allocation index, a commonly used composite measure previously implicated in tobacco smoking(12). Further, default mode network connectivity was relatively increased during satiated versus deprived states, and connectivity within canonical networks was unrelated to subjective craving and withdrawal measures. These findings differ from prior work using cross-over designs to compare smokers during abstinent versus satiated states over longer periods of time (i.e., scans conducted days to weeks apart)(12), but are nonetheless consistent with prior work on acute effects of nicotine administration (i.e., same day scans conducted before and after acute nicotine)(14). Taken together, these data raise the possibility of differential effects of acute versus chronic smoking satiation on large scale network dynamics. However, as the networks used here were not defined using independent component analysis (ICA), as in prior smoking studies focusing on canonical networks, further research directly comparing across different states (abstinence, reinstatement, smoking-as-usual) and analysis approaches is needed to clarify the role of default mode, salience and frontoparietal network dynamics in smoking behaviors.

Consistent with our second hypothesis, whole-brain, intrinsic connectivity comparisons identified between-group differences in connectivity within distributed neural systems that were smoking state dependent. Specifically, in comparison to nonsmokers, smokers during deprivation exhibited increased connectivity within the cerebellum, hippocampus and striatum. With the exception of the striatum, these alterations were attenuated following smoking reinstatement, indicating possibly normalizing effects of tobacco use on intrinsic patterns of connectivity among smokers. Consistent with this interpretation, residual craving and withdrawal symptoms following smoking reinstatement were positively associated with connectivity within hippocampal and cerebellar regions, such that smokers continuing to experience subjective craving/withdrawal symptoms had elevated connectivity within these regions. Notably, these data are consistent with diffusion data demonstrating direct connections between the limbic system and cerebellum(50). Collectively, these data

therefore indicate that smoking deprivation is characterized by greater subcortical and cerebellar connectivity and that connectivity within these regions encodes for individual differences in subjective craving and withdrawal during satiation.

While the cerebellum has not been a primary focus of prior studies assessing connectivity across smoking states, substantial literature indicates cerebellar involvement in tobacco use behaviors (and in addictions more generally)(51, 52). The cerebellum is characterized by a wide distribution of nAchRs, including those sensitive to nicotinic sensitization (e.g., $\alpha 4\beta 2$ subunit-containing nAchRs)(7, 21, 53), and reductions in cerebellar gray matter have been frequently reported among smokers(21, 54–57). In addition, recent neuroanatomical work indicates dense reciprocal cerebellar connections to cortical and subcortical regions —including direct connections between the striatum and cerebellum—providing the anatomical basis for cerebellar involvement in diverse behaviors beyond simple motor control and coordination(58, 59). Within this context, striatal-cerebellar connections are theorized to contribute to associative reward learning processes (including automatization of drug behaviors) and cortico-cerebellar connections are posited to contribute to craving via encoding of predicted internal and external states(59–61).

Consistent with the above theoretical framework, seed-to-voxel analyses indicated significantly increased within-cerebellum connectivity and decreased corticostriatal-cerebellar connectivity among smokers (relative to non-smokers) during deprivation, which were partially ameliorated following smoking reinstatement. This included increased connectivity between the cerebellum and regions previously implicated in smoking behaviors, e.g., anterior cingulate, medial PFC, right caudate(62–64). As the anterior cingulate is a central component of the salience network, this finding partially aligns with our network-of-interest analysis indicating decreased salience network connectivity among smokers across smoking states, but suggests that this canonical network finding might also extend to include more distributed cerebellar systems. Taken together with findings of increased intra-cerebellar connectivity, these data further raise the possibility that decreased connectivity between corticostriatal and cerebellar systems may reflect a reallocation of cerebellar resources away from the cortex during abstinence that may be compensatory in nature. While speculative, this interpretation is consistent with the hypothesized role of cingulo-cerebellar networks in drug craving(60), with recent work implicating the cerebellum in relapse risk during a quit-attempt(51), and with our findings of smoking state dependent effects on connectivity within these regions. However, further research is needed to assess the potential efficacy of interventions directly targeting cerebellar connectivity (e.g., via neurofeedback or pharmacotherapy) during early abstinence to prevent smoking reinstatement(51, 65, 66). Similarly, additional work is needed to determine the extent to which cerebellar findings are simply reflective of large scale network activity (67).

This study has several strengths, including use of both a within- and between-subjects design to assess the effects of smoking state on intrinsic connectivity comparisons of smokers versus nonsmokers in a data driven manner. To our knowledge, this is largest within-subjects study of functional connectivity across smoking states to also include a control group, thereby enabling determination of whether connectivity changes in smokers represent a restoration to (i.e., return to premorbid levels)—or deviation from

(i.e., alteration from premorbid levels)—typical patterns of intrinsic connectivity(13). This study also has limitations, including significant age differences between smoking and non-smoking participant groups. However, all of our primary between-group findings remained significant in follow-up analyses controlling for age. In addition, as between-group differences in connectivity were largely smoking state dependent, it is unlikely that this variable was a primary contributor to observed differences in connectivity. Other significant limitations include a relatively short duration of resting state data acquired relative to recent recommendations(37), no maximum cut-off for CO levels on abstinent scan days, limited information on co-occurring other substance use for smoking and non-smoking participants, no data on potential acute effects of other substances and the small number of female participants in smoking group (n=10), which precluded us from assessing sex effects. Finally, some findings related to canonical networks (i.e., NOI-based approach) were no longer significant following inclusion of residual motion as a covariate, likely due to a reduction in statistical power (68). These data nonetheless for the first time demonstrate significant effects of smoking state on whole-brain intrinsic connectivity comparisons and identify novel targets for intervention strategies (e.g., neurofeedback) aimed at increasing abstinence early-on in a quit attempt. They indicate that future studies of nicotine effects should consider network dynamics at the whole-brain level, rather than focusing solely on frontoparietal, salience and default mode networks.

Supplementary Material

Refer to Web version on PubMed Central for supplementary material.

Acknowledgments:

The authors thank the Core for Advanced MRI (CAMRI) at Baylor College of Medicine and Dr. Dustin Scheinost for help with ICD analyses.

Funding and disclosures: This study was supported by Veterans Health Administration VHA5I01CX000994 and VHA1I21RX002588, National Institute on Drug Abuse grants K01DA039299, T32DA022975, R03DA029167 and K01DA026539. Dr. Abdallah has served as a consultant and speaker and/or on advisory boards for Janssen, Lundbeck, Psilocybin Lab and FSV7 and editor of *Chronic Stress* for Sage Publications, Inc. and filed a patent for using mTORC1 inhibitors to augment the effects of antidepressants (filed on Aug 20, 2018). All other authors have no disclosures.

References

1. USDHHS, The Health Consequences of Smoking—50 Years of Progress: A Report of the Surgeon General 2014: Atlanta, GA.
2. Grant B, Hasin DS, Chou SP, Stinson FS, Dawson DA (2004): Nicotine dependence and psychiatric disorders in the United States: results from the national epidemiologic survey on alcohol and related conditions. Arch Gen Psychiatry 61: 1226–1233. [PubMed: 15583114]
3. Li XH, An FR, Ungvari GS, Ng CH, Chiu HFK, Wu PP, et al. (2017): Prevalence of smoking in patients with bipolar disorder, major depressive disorder and schizophrenia and their relationships with quality of life. Sci Rep 7(1): 8430. [PubMed: 28814728]
4. Cahill K, Stevens S, Perera R, Lancaster T (2013): Pharmacological interventions for smoking cessation: an overview and network meta-analysis. The Cochrane database of systematic reviews 5: Cd009329.

5. Yip S, Carroll K, Potenza M, An overview of translational approaches to the treatment of addictions, in Neuroimaging and Psychosocial Addiction Treatment: An Integrative Guide for Researchers and Clinicians, Feldstein Ewing S, Witkiewitz K, and Filbey F, Editors. 2015, Palgrave.
6. Fedota JR, Ding X, Matous AL, Salmeron BJ, McKenna MR, Gu H, et al. (2018): Nicotine Abstinence Influences the Calculation of Salience in Discrete Insular Circuits. Biological psychiatry. Cognitive neuroscience and neuroimaging 3(2): 150–159. [PubMed: 29529410]
7. Gotti C, Clementi F, Fornari A, Gaimarri A, Guiducci S, Manfredi I, et al. (2009): Structural and functional diversity of native brain neuronal nicotinic receptors. Biochemical pharmacology 78(7): 703–11. [PubMed: 19481063]
8. Fedota JR, Stein EA (2015): Resting-state functional connectivity and nicotine addiction: prospects for biomarker development. Ann N Y Acad Sci 1349(1): 64–82. [PubMed: 26348486]
9. Bi Y, Zhang Y, Li Y, Yu D, Yuan K, Tian J (2017): 12h abstinence-induced right anterior insula network pattern changes in young smokers. Drug Alcohol Depend 176: 162–168. [PubMed: 28544994]
10. Perry RN, Schlagintweit HE, Darredeau C, Helmick C, Newman AJ, Good KP, Barrett SP (2020): Corrigendum to The impacts of actual and perceived nicotine administration on insula functional connectivity with the anterior cingulate cortex and nucleus accumbens. J Psychopharmacol 34(5): 588. [PubMed: 32013675]
11. Ding X, Lee SW (2013): Changes of functional and effective connectivity in smoking replenishment on deprived heavy smokers: a resting-state FMRI study. PLoS One 8(3): e59331. [PubMed: 23527165]
12. Lerman C, Gu H, Loughead J, Ruparel K, Yang Y, Stein EA (2014): Large-scale brain network coupling predicts acute nicotine abstinence effects on craving and cognitive function. JAMA psychiatry 71(5): 523–30. [PubMed: 24622915]
13. Garavan H, Brennan KL, Hester R, Whelan R (2013): The neurobiology of successful abstinence. Curr Opin Neurobiol 23(4): 668–74. [PubMed: 23510740]
14. Tanabe J, Nyberg E, Martin LF, Martin J, Cordes D, Kronberg E, Tregellas JR (2011): Nicotine effects on default mode network during resting state. Psychopharmacol (Berl) 216(2): 287–95.
15. Zhao S, Li Y, Li M, Wang R, Bi Y, Zhang Y, et al. (2019): 12-h abstinence-induced functional connectivity density changes and craving in young smokers: a resting-state study. Brain imaging and behavior 13(4): 953–962. [PubMed: 29926324]
16. Wang C, Zhang Y, Yan C, Sun M, Cheng J (2018): The thalamo-cortical resting state functional connectivity and abstinence-induced craving in young smokers. Brain imaging and behavior 12(5): 1450–1456. [PubMed: 29297152]
17. Scheinost D, Benjamin J, Lacadie CM, Vohr B, Schneider KC, Ment LR, et al. (2012): The intrinsic connectivity distribution: a novel contrast measure reflecting voxel level functional connectivity. Neuroimage 62(3): 1510–9. [PubMed: 22659477]
18. Qiu M, Scheinost D, Ramani R, Constable RT (2017): Multi-modal analysis of functional connectivity and cerebral blood flow reveals shared and unique effects of propofol in large-scale brain networks. NeuroImage 148: 130–140. [PubMed: 28069540]
19. Garrison KA, Scheinost D, Finn ES, Shen X, Constable RT (2015): The (in)stability of functional brain network measures across thresholds. Neuroimage 118: 651–61. [PubMed: 26021218]
20. Garrison KA, Sinha R, Lacadie CM, Scheinost D, Jastreboff AM, Constable RT, Potenza MN (2016): Functional Connectivity During Exposure to Favorite-Food, Stress, and Neutral-Relaxing Imagery Differs Between Smokers and Nonsmokers. Nicotine & tobacco research : official journal of the Society for Research on Nicotine and Tobacco 18(9): 1820–9. [PubMed: 26995796]
21. Shen Z, Huang P, Wang C, Qian W, Yang Y, Zhang M (2018): Cerebellar Gray Matter Reductions Associate With Decreased Functional Connectivity in Nicotine-Dependent Individuals. Nicotine & tobacco research : official journal of the Society for Research on Nicotine and Tobacco 20(4): 440–447. [PubMed: 29065207]
22. Wall MB, Mentink A, Lyons G, Kowalczyk OS, Demetriou L, Newbould RD (2017): Investigating the neural correlates of smoking: Feasibility and results of combining electronic cigarettes with fMRI. Sci Rep 7(1): 11352. [PubMed: 28900267]

23. Placzek AN, Molfese DL, Khatiwada S, Viana Di Prisco G, Huang W, Sidrauski C, et al. (2016): Translational control of nicotine-evoked synaptic potentiation in mice and neuronal responses in human smokers by eIF2α. eLife 5.
24. Qian DC, Molfese DL, Jin JL, Titus AJ, He Y, Li Y, et al. (2017): Genome-wide imaging association study implicates functional activity and glial homeostasis of the caudate in smoking addiction. BMC genomics 18(1): 740. [PubMed: 28927378]
25. Yip SW, Scheinost D, Potenza MN, Carroll KM (2019): Connectome-based prediction of cocaine abstinence. American Journal of Psychiatry 175(2): 156–164.
26. Fagerstrom KO (1978): Measuring degree of physical dependence to tobacco smoking with reference to individualization of treatment. Addict Behav 3(3–4): 235–41. [PubMed: 735910]
27. McClernon F, Hiott F, Huettel S, Rose J (2005): Abstinence-induced changes in self-report craving correlate with event-realted fMRI responses to smoking cues. Neurpsychopharmacology 30(1940–7).
28. Shiffman S, West R, Gilbert D (2004): Recommendation for the assessment of tobacco craving and withdrawal in smoking cessation trials. Nicotine & tobacco research : official journal of the Society for Research on Nicotine and Tobacco 6(4): 599–614. [PubMed: 15370156]
29. Rosenberg MD, Finn ES, Scheinost D, Papademetris X, Shen X, Constable RT, Chun MM (2016): A neuromarker of sustained attention from whole-brain functional connectivity. Nat Neurosci 19(1): 165–71. [PubMed: 26595653]
30. Rosenberg MD, Zhang S, Hsu WT, Scheinost D, Finn ES, Shen X, et al. (2016): Methylphenidate Modulates Functional Network Connectivity to Enhance Attention. J Neurosci 36(37): 9547–57. [PubMed: 27629707]
31. Finn ES, Shen X, Scheinost D, Rosenberg MD, Huang J, Chun MM, et al. (2015): Functional connectome fingerprinting: identifying individuals using patterns of brain connectivity. Nat Neurosci 18(11): 1664–71. [PubMed: 26457551]
32. Joshi A, Scheinost D, Okuda H, Belhachemi D, Murphy I, Staib LH, Papademetris X (2011): Unified framework for development, deployment and robust testing of neuroimaging algorithms. Neuroinformatics 9(1): 69–84. [PubMed: 21249532]
33. Satterthwaite TD, Elliott MA, Gerraty RT, Ruparel K, Loughead J, Calkins ME, et al. (2013): An improved framework for confound regression and filtering for control of motion artifact in the preprocessing of resting-state functional connectivity data. Neuroimage 64: 240–56. [PubMed: 22926292]
34. Shen X, Finn ES, Scheinost D, Rosenberg MD, Chun MM, Papademetris X, Constable RT (2017): Using connectome-based predictive modeling to predict individual behavior from brain connectivity. Nat. Protocols 12(3): 506–518. [PubMed: 28182017]
35. Buckner RL, Sepulcre J, Talukdar T, Krienen FM, Liu H, Hedden T, et al. (2009): Cortical hubs revealed by intrinsic functional connectivity: mapping, assessment of stability, and relation to Alzheimer's disease. J Neurosci 29(6): 1860–73. [PubMed: 19211893]
36. Horien C, Shen X, Scheinost D, Constable RT The individual functional connectome is unique and stable over months to years. NeuroImage 189: 676–687. [PubMed: 30721751]
37. Noble S, Spann M, Tokoglu F, Shen X, Constable R, Scheinost D (2017): Influences on the test-retest reliability of functional connectivity MRI and its relationship with behavioral utility. Cereb Cortex 27(11): 5415–5429. [PubMed: 28968754]
38. Finn ES, Shen X, Scheinost D, Rosenberg MD, Huang J, Chun MM, et al. (2015): Functional connectome fingerprinting: identifying individuals using patterns of brain connectivity. Nat Neurosci
39. Scheinost D, Finn ES, Tokoglu F, Shen X, Papademetris X, Hampson M, Constable RT (2015): Sex differences in normal age trajectories of functional brain networks. Hum Brain Mapp 36(4): 1524–35. [PubMed: 25523617]
40. Zakiniaeiz Y, Scheinost D, Seo D, Sinha R, Constable RT (2017): Cingulate cortex functional connectivity predicts future relapse in alcohol dependent individuals. NeuroImage Clin 13: 181–187. [PubMed: 27981033]
41. Mitchell MR, Balodis IM, Devito EE, Lacadie CM, Yeston J, Scheinost D, et al. (2013): A preliminary investigation of Stroop-related intrinsic connectivity in cocaine dependence:

associations with treatment outcomes. Am J Drug Alcohol Abuse 39(6): 392–402. [PubMed: 24200209]

42. Scheinost D, Kwon SH, Lacadie C, Vohr BR, Schneider KC, Papademetris X, et al. (2017): Alterations in Anatomical Covariance in the Prematurely Born. Cereb Cortex 27(1): 534–543. [PubMed: 26494796]
43. Gu X, Lohrenz T, Salas R, Baldwin PR, Soltani A, Kirk U, et al. (2016): Belief about Nicotine Modulates Subjective Craving and Insula Activity in Deprived Smokers. Front Psychiatry 7: 126. [PubMed: 27468271]
44. Gu X, Lohrenz T, Salas R, Baldwin PR, Soltani A, Kirk U, et al. (2015): Belief about nicotine selectively modulates value and reward prediction error signals in smokers. Proc Natl Acad Sci U S A 112(8): 2539–44. [PubMed: 25605923]
45. Cole DM, Beckmann CF, Long CJ, Matthews PM, Durcan MJ, Beaver JD (2010): Nicotine replacement in abstinent smokers improves cognitive withdrawal symptoms with modulation of resting brain network dynamics. Neuroimage 52(2): 590–9. [PubMed: 20441798]
46. Hobkirk AL, Nichols TT, Foulds J, Yingst JM, Veldheer S, Hrabovsky S, et al. (2018): Changes in resting state functional brain connectivity and withdrawal symptoms are associated with acute electronic cigarette use. Brain Res Bull 138: 56–63. [PubMed: 28528203]
47. Li Y, Yuan K, Bi Y, Guan Y, Cheng J, Zhang Y, et al. (2017): Neural correlates of 12-h abstinence-induced craving in young adult smokers: a resting-state study. Brain Imaging Behav 11(3): 677–684. [PubMed: 26995747]
48. Sutherland MT, McHugh M, Pariyadath V, Stein EA (2012): Resting State Functional Connectivity in Addiction: Lessons Learned and a Road Ahead. NeuroImage 62(4): 2281–2295. [PubMed: 22326834]
49. Pariyadath V, Gowin JL, Stein EA, Chapter 8 - Resting state functional connectivity analysis for addiction medicine: From individual loci to complex networks, in Progress in brain research, Hamed E and Martin PP, Editors. 2016, Elsevier. p. 155–173.
50. Arrigo A, Mormina E, Anastasi GP, Gaeta M, Calamuneri A, Quartarone A, et al. (2014): Constrained spherical deconvolution analysis of the limbic network in human, with emphasis on a direct cerebello-limbic pathway. Front Hum Neurosci 8: 987. [PubMed: 25538606]
51. Shen Z, Huang P, Wang C, Qian W, Yang Y, Zhang M (2017): Increased network centrality as markers of relapse risk in nicotine-dependent individuals treated with varenicline. Progress in neuro-psychopharmacology & biological psychiatry 75: 142–147. [PubMed: 28185963]
52. Moreno-Rius J (2019): Opioid addiction and the cerebellum. Neuroscience and biobehavioral reviews 107: 238–251. [PubMed: 31526817]
53. Paterson D, Nordberg A (2000): Neuronal nicotinic receptors in the human brain. Prog Neurobiol 61(1): 75–111. [PubMed: 10759066]
54. Sutherland MT, Riedel MC, Flannery JS, Yanes JA, Fox PT, Stein EA, Laird AR (2016): Chronic cigarette smoking is linked with structural alterations in brain regions showing acute nicotinic drug-induced functional modulations. Behavioral and brain functions : BBF 12(1): 16. [PubMed: 27251183]
55. Franklin TR, Wetherill RR, Jagannathan K, Johnson B, Mumma J, Hager N, et al. (2014): The effects of chronic cigarette smoking on gray matter volume: influence of sex. PLoS One 9(8): e104102. [PubMed: 25090480]
56. Kuhn S, Romanowski A, Schilling C, Mobascher A, Warbrick T, Winterer G, Gallinat J (2012): Brain grey matter deficits in smokers: focus on the cerebellum. Brain structure & function 217(2): 517–22. [PubMed: 21909705]
57. Wetherill RR, Jagannathan K, Hager N, Childress AR, Rao H, Franklin TR (2015): Cannabis, Cigarettes, and Their Co-Occurring Use: Disentangling Differences in Gray Matter Volume. The international journal of neuropsychopharmacology / official scientific journal of the Collegium Internationale Neuropsychopharmacologicum (CINP) 18(10): pyv061.
58. Strick PL, Dum RP, Fiez JA (2009): Cerebellum and nonmotor function. Annual review of neuroscience 32: 413–34.
59. Bostan AC, Dum RP, Strick PL (2013): Cerebellar networks with the cerebral cortex and basal ganglia. Trends Cogn Sci 17(5): 241–54. [PubMed: 23579055]

60. Moreno-Rius J, Miquel M (2017): The cerebellum in drug craving. Drug Alcohol Depend 173: 151–158. [PubMed: 28259088]

61. Grant S, London ED, Newlin DB, Villemagne VL, Liu X, Contoreggi C, et al. (1996): Activation of memory circuits during cue-elicited cocaine craving. Proc Natl Acad Sci U S A 93: 12040–12045. [PubMed: 8876259]

62. Janes AC, Farmer S, Peechatka AL, Frederick Bde B, Lukas SE (2015): Insula-Dorsal Anterior Cingulate Cortex Coupling is Associated with Enhanced Brain Reactivity to Smoking Cues. Neuropsychopharmacol 40(7): 1561–8.

63. Janes AC, Park MT, Farmer S, Chakravarty MM (2015): Striatal morphology is associated with tobacco cigarette craving. Neuropsychopharmacol 40(2): 406–11.

64. Yuan K, Zhao M, Yu D, Manza P, Volkow ND, Wang GJ, Tian J (2018): Striato-cortical tracts predict 12-h abstinence-induced lapse in smokers. Neuropsychopharmacol 43(12): 2452–2458.

65. Hartwell KJ, Hanlon CA, Li X, Borckardt JJ, Canterberry M, Prisciandaro JJ, et al. (2016): Individualized real-time fMRI neurofeedback to attenuate craving in nicotine-dependent smokers. J. Psychiatry Neurosci 41(1): 48–55. [PubMed: 26505139]

66. Li X, Hartwell KJ, Borckardt J, Prisciandaro JJ, Saladin ME, Morgan PS, et al. (2013): Volitional reduction of anterior cingulate cortex activity produces decreased cue craving in smoking cessation: a preliminary real-time fMRI study. Addict Biol 18(4): 739–48. [PubMed: 22458676]

67. Habas C, Kamdar N, Nguyen D, Prater K, Beckmann CF, Menon V, Greicius MD (2009): Distinct cerebellar contributions to intrinsic connectivity networks. J Neurosci 29(26): 8586–94. [PubMed: 19571149]

68. Satterthwaite TD, Ciric R, Roalf DR, Davatzikos C, Bassett DS, Wolf DH (2019): Motion artifact in studies of functional connectivity: Characteristics and mitigation strategies. Hum Brain Mapp 40(7): 2033–2051. [PubMed: 29091315]

69. Shen X, Tokoglu F, Papademetris X, Constable RT (2013): Groupwise whole-brain parcellation from resting-state fMRI data for network node identification. Neuroimage 82: 403–15. [PubMed: 23747961]

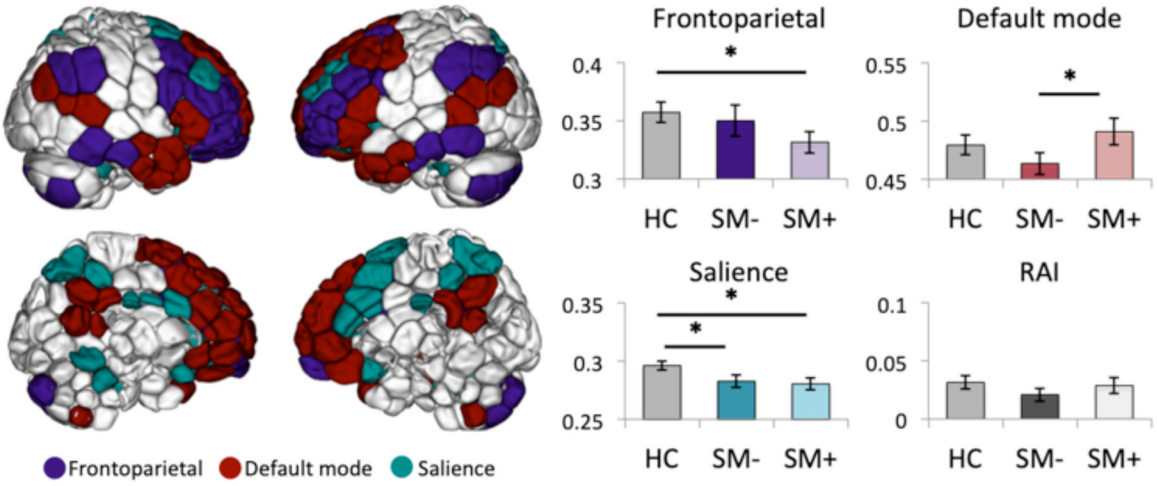

Figure 1 –. Canonical network and resource allocation index comparisons of non-smokers versus smokers during deprived and satiated states

Left: Lateral (top) and medial (bottom) maps showing node definitions for frontoparietal, default mode and salience networks. Nodes were defined using the Shen-268 parcellation and canonical networks were defined based on prior work(37, 38, 69). Right: Mean±standard error canonical network and resource allocation index (RAI) strengths are plotted for healthy controls (HC), deprived smokers (SM-) and satiated smokers (SM+).

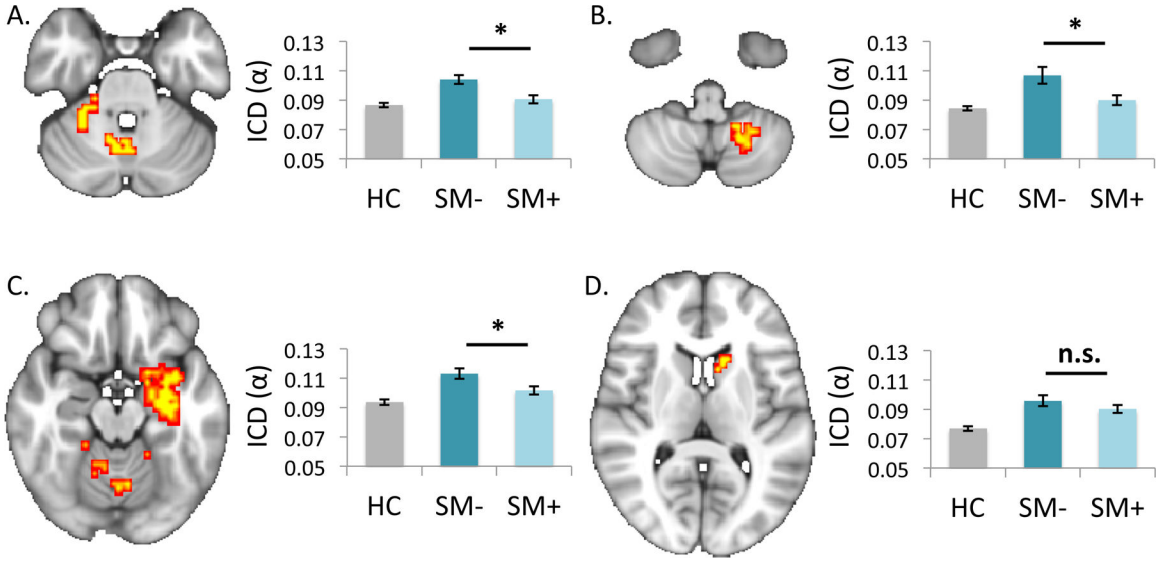

Figure 2 –. Whole-brain intrinsic connectivity comparisons of non-smokers versus smokers during deprived and satiated states

Statistical maps show findings from whole-brain intrinsic connectivity distribution (ICD) comparisons of healthy controls versus deprived smokers (pTFCE<.01). Corresponding cluster values for healthy controls (HC), deprived smokers (SM-) and satiated smokers (SM+) are plotted for (a) right and (b) left cerebellar clusters and for (c) right hippocampal and (d) left striatal clusters. Post-hoc analyses indicated significant decreases in connectivity with cerebellar and hippocampal regions following smoking reinstatement. Images are shown in radiological convention (left=right). *p<.05; n.s.=not significant (p>.05).

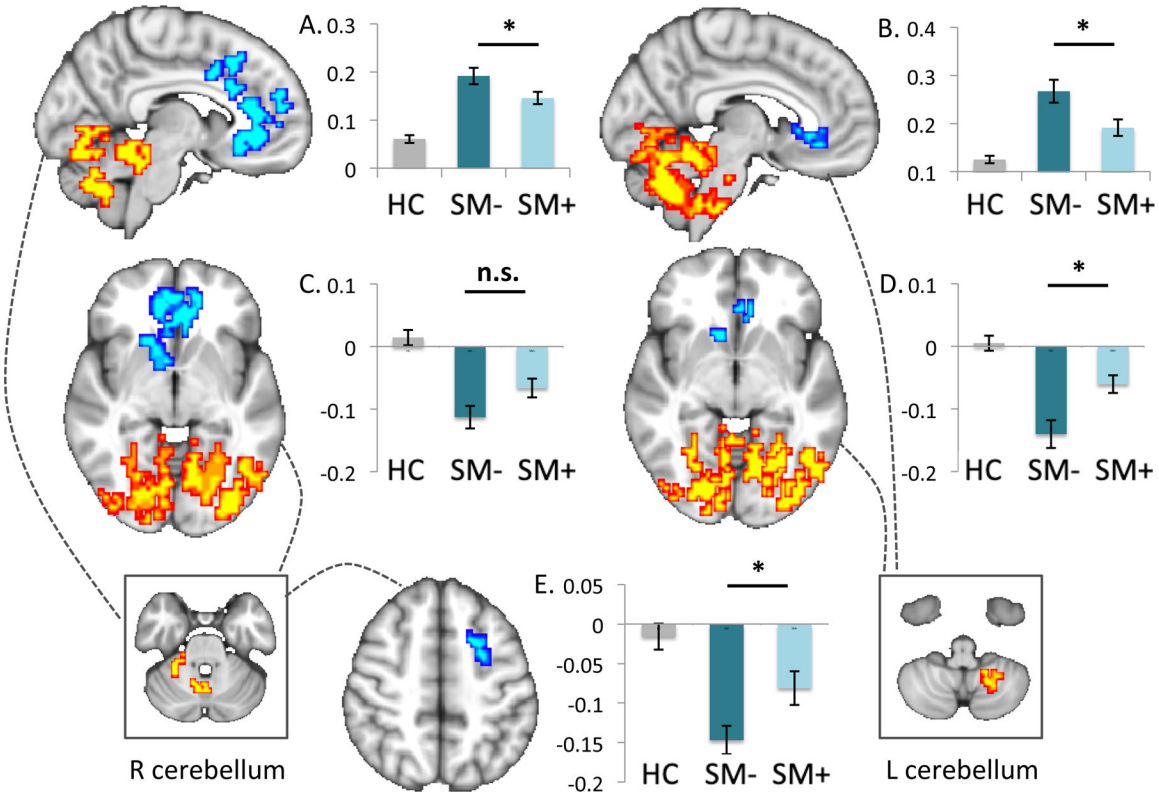

Figure 3 –. Seed-based connectivity comparisons of non-smokers versus smokers during deprived and satiated states

Findings from seed-based connectivity analyses (pTFCE<.05) using clusters identified in whole-brain intrinsic connectivity distribution (ICD) comparisons of deprived smokers versus healthy controls are shown for the right and left cerebellar seeds (boxes at bottom) with dotted lines indicating resultant whole-brain maps. Cluster values for healthy controls, deprived and satiated smokers are plotted for cerebellar clusters (top, a, b), corticostriatal clusters (middle, c, d) and for the medial PFC (bottom, e). The y-axis indicates α. Images are shown in radiological convention (left=right). *p<.05; n.s.=not significant (p>.05).

Table 1 –

Whole-brain and seed-to-voxel intrinsic connectivity distribution (ICD) findings

Whole-brain connectivity		**k**	**p**	**x**	**y**	**z**
Deprived Smokers > Nonsmokers						
C1	L hippocampus, parahippocampus, amygdala, temporal pole, L & R cerebellum	383	.002	−30	−9	−21
C2	L & R cerebellum I-V	116	.004	24	−36	−30
C3	L cerebellum VIIIb, IX, Vllla	30	.005	−18	−54	−48
C4	L caudate	21	.005	−15	12	15
Seed-to-voxel connectivity		**k**	**p**	**x**	**y**	**z**
Deprived Smokers > Nonsmokers						
C1	—					
C2	L & R cerebellum, occipital, precuneus	2231	<.001	−21	−54	−15
C3	L & R cerebellum, occipital, brainstem	2434	<.001	18	−81	−45
C4	—					
Deprived Smokers < Nonsmokers						
C1	—					
C2	Anterior cingulate, medial PFC	693	.002	15	39	−3
C2	R caudate, putamen, subgenual	48	.011	−24	9	48
C3	R accumbens, caudate, putamen, anterior cingulate	112	.011	18	21	0
C4	—					

Whole-brain connectivity (top): Cluster descriptions, cluster size (k), peak p-values and peak MNI coordinates are shown for clusters identified in whole-brain ICD analyses of nonsmokers and smokers during deprivation. No clusters were identified as significant in whole-brain analyses comparing nonsmokers and smokers during satiation.

Seed-to-voxel connectivity (bottom): Cluster descriptions, cluster size (k), peak p-values and peak MNI coordinates are shown for clusters identified in follow-up seed-based analyses (using clusters identified in whole-brain comparisons, above) of nonsmokers and smokers during deprivation. Seed-to-voxel analyses for the left hippocampus (C1) and caudate (C4) clusters did not identify any specific regions as primary contributors whole-brain alterations, indicating that connectivity increases for these regions were diffuse in nature (i.e., not localized to a single connection).

Biol Psychiatry Cogn Neurosci Neuroimaging. Author manuscript; available in PMC 2023 September 01.